

The following pages constitute the final, accepted and revised manuscript of the article:

Andersson Nordahl, Emma and Rydengård, Victoria and Mörgelin, Matthias and Schmidtchen, Artur

“Domain 5 of high molecular weight kininogen is antibacterial”

J Biol Chem. 2005 Oct 14;280(41):34832-9.

Publisher: American Society for Biochemistry and Molecular Biology

Use of alternative location to go to the published version of the article requires journal subscription.

Alternative location: <http://dx.doi.org/10.1074/jbc.M507249200>

DOMAIN 5 OF HIGH MOLECULAR WEIGHT KININOGEN IS ANTIBACTERIAL*

Emma Andersson Nordahl‡ ||, Victoria Rydengård‡,
Matthias Mörgelin¶, and Artur Schmidtchen‡

From the Department of Clinical Sciences, Lund, ‡Section of Dermatology and Venereology and ¶Section of Clinical and Experimental Infectious Medicine, Lund University, Biomedical Center, Tornavägen 10, SE-221 84 Lund, Sweden.

Running Title: Antimicrobial activity of domain 5 of HMWK

|| To whom correspondence should be addressed: Emma Andersson Nordahl, Department of Clinical Sciences, Lund, Biomedical Center B14, Tornavägen 10, SE-221 84 Lund, Sweden, Tel: +46 46 120921, Fax: +46 46 157756, E-Mail: emma.nordahl@med.lu.se

Antimicrobial peptides are important effectors of the innate immune system. These peptides belong to a multifunctional group of molecules that apart from their antibacterial activities also interact with mammalian cells, glycosaminoglycans, and control chemotaxis, apoptosis, and angiogenesis. Here we demonstrate a novel antimicrobial activity of the heparin-binding and cell-binding domain 5 of high molecular weight kininogen. Antimicrobial epitopes of domain 5 were characterized by analysis of overlapping peptides. A peptide, HKH20 (H479-H498), efficiently killed the Gram-negative bacteria *Escherichia coli*, *Pseudomonas aeruginosa*, and the Gram-positive *Enterococcus faecalis*. Fluorescence microscopy and electron microscopy demonstrated that HKH20 binds to and induces breaks in bacterial membranes. Furthermore, no discernible hemolysis, or membrane permeabilizing effects on eukaryotic cells, were noted. Proteolytic degradation of high molecular weight kininogen by neutrophil-derived proteases as well as the metalloproteinase elastase from *Pseudomonas aeruginosa* yielded fragments comprising HKH20 epitopes, indicating that kininogen-derived antibacterial peptides are released during proteolysis.

The innate immune system, based on antimicrobial peptides (AMP)¹, provides a rapid and non-specific response against potentially invasive pathogenic microorganisms. AMPs, first isolated from human leukocyte extracts by Zeya and Spitznagel in 1963 (1), were subsequently discovered in invertebrates (2) and cold-blooded

vertebrates (3). At present, over 880 different AMPs have been identified in eukaryotes (www.bbcm.univ.trieste.it/~tossi/pag5.htm).

During recent years it has become increasingly evident that many antimicrobial peptides are multifunctional (4,5). They are found to mediate chemotaxis (LL-37, defensins)(6-8), apoptosis (lactoferrin, LL-37) (9-11), and angiogenesis (PR-39, LL-37) (12,13). Conversely, molecules previously not considered as AMPs, including proinflammatory and chemotactic chemokines (14), neuropeptides (15-19) and peptide hormones (16,20), have recently been found to exert antibacterial activities. The proinflammatory, chemotactic and anaphylatoxic peptide C3a, generated during activation of the complement system displays potent antibacterial effects (21). Many AMPs, by virtue of their cationicity and amphipathicity, also interact with heparin (22,23).

High molecular weight kininogen (HMWK) is a multifunctional 120 kDa glycoprotein found in plasma (~80 µg/ml) (24) and in α-granules of platelets (25). The protein is composed of six domains, each having different properties and specific ligands (24). Domains D1-D3 have a cystatin-like structure, and the two latter domains serve as specific inhibitors of cysteine proteinases such as cathepsins and calpains. The D4 domain contains the bradykinin sequence, which is released by plasma kallikreins during contact activation (24,26). Biologically active kinins can also be generated by the cooperative action of mast cell tryptase and neutrophil elastase (27). Thus, similar to complement degradation, limited proteolysis of HMWK generates highly vasocative and proinflammatory peptides, which are formed at sites of tissue

injury and inflammation. The heparin-binding (28), cell-binding (29) and antiangiogenic (30) D5 from HMWK, contains regions dominated by histidine, glycine, and in certain parts, interspersed lysine residues (31). The starting point for this study was the observation that this domain of HMWK shares many structural (cationicity, spacing of basic residues) and functional features with AMPs. Here we show that recombinant domain 5 (rD5), related peptide epitopes, as well as HMWK cleavage products function as "classical" AMPs, thus disclosing a previously unknown antibacterial activity of domain 5 of HMWK.

EXPERIMENTAL PROCEDURE

Biological materials – Blood drawn from healthy volunteers (Vacutainer tubes, Becton, Dickinson & Co, containing 2 mg/ml K3EDTA) was used for preparation of erythrocytes and EDTA plasma. For preparation of citrate plasma vacutainer tubes containing 1:9 (v/v), 129 mM sodium citrate, were used. The plasma was separated from the blood by centrifugation at 2500 g in 15 min. The pellet was removed and plasma samples were stored at -20°C . HaCaT keratinocytes were kindly provided by Dr. Robert Fusenig (Heidelberg University, Germany) and were cultured in DMEM containing 5.5 mM glucose and 10% fetal calf serum (FCS). Polyclonal rabbit antibodies raised against HKH20 were purchased from Innovagen AB, Lund, Sweden. Neutrophils were prepared by routine procedures (polymorphprepTM, AXIS-SHIELD PoC AS, Oslo, Norway) from blood of healthy human donors. The cells were disrupted by freeze thawing and addition of 0.3% Tween 20.

Peptides/Proteins and enzymes – HMWK was obtained from the Binding site inc. (San Diego, CA, USA). The synthetic peptides: KHN20, GHG20, GHG21, GGH20, HKH20, LDD40, Texas Red conjugated HKH20, GKH17 (Fig. 1B) and LL-37 (LLGDFFRKSKEK-IGKEFKRIVQRIKDFLRNLPRTES) were synthesized by Innovagen AB. The purity (>95%) and molecular weight of these peptides was confirmed by mass spectral analysis (MALDI-TOF Voyager, Applied Biosystems, Foster City, CA, USA). Neutrophil serine protease, human leukocyte elastase (HLE) (0.2 $\mu\text{g}/\mu\text{l}$, 5.8 $\text{mu}/\mu\text{l}$) and *Pseudomonas aeruginosa* elastase (0.05 $\mu\text{g}/\mu\text{l}$, 13.05 $\text{mu}/\mu\text{l}$) were obtained from Calbiochem (San Diego, CA,

USA). An equivalent *Pseudomonas aeruginosa* elastase (62 $\text{mu}/\mu\text{l}$) was kindly provided by Dr. H. Maeda, Kumamoto University, Japan.

Purification of the recombinant domain 5 – The expression vector (pET25b) (Novagen, Inc., Madison, WI, USA) containing rD5 was expressed in *Escherichia coli* strain BL21(DE3) generously provided by Dr. U. Sjöbring (32). One millimolar isopropyl thio- β -D-galactoside was added to exponentially growing bacteria to induce protein production. After 3 h incubation at 30°C , bacteria were harvested by centrifugation (2800 g for 10 min) and the pellet was resuspended in 3 ml sonication buffer (s-buffer: 50 mM phosphate, 300 mM NaCl, pH 8.0). The bacteria were lysed by repeated cycles of freeze thawing. The lysate was centrifuged at 30000 g for 30 min and the supernatant was mixed with 2 ml Ni/nitrilotriacetic acid Sepharose (QIAGEN GmbH, Hilden, Germany) equilibrated with s-buffer and incubated on rotation for 1 h at room temperature. The Sepharose gel was loaded into a column and washed with 10 ml s-buffer containing 0.1% (v/v) Triton X-100, 10 ml s-buffer, 5 ml s-buffer with 1 M NaCl, 5 ml s-buffer, 10 ml 20% ethanol, 10 ml s-buffer containing 5 mM imidazole and finally 10 ml s-buffer with 30 mM imidazole. The rD5 protein was eluted with s-buffer containing 500 mM imidazole.

Molecular modeling – A model structure of rD5 (Fig. 1A) was created based on the homologous protein hisactophilin from *Dictyostelium discoideum* (Protein Data Bank code 1HCE (33)). The sequence of human rD5 (residues 414-525) was aligned against the sequence of hisactophilin using the alignment described in (34). The modeling was performed using the Prime module (35) from the Schrödinger computational chemistry suite of programs (Schrödinger, L.L.C., Portland, OR, USA). The sequence identity was 32% and rotamers from the conserved residues was retained. Terminal tails and residues not derived from the template were minimized during structure building. All loops were refined one at a time using default sampling in the loop refinement protocol built into Prime. Most of the backbone torsion angles for non-glycine residues lie within allowed regions of the Ramachandran plot. The few non-glycine residues outside these regions (Trp 18, Gln 38 and His 92) are located in loop regions.

Microorganisms – *Escherichia coli* strain BL21(DE3) was used for expression of the rD5

containing vector. *Escherichia coli* 37.4, *Enterococcus faecalis* 2374 and *Pseudomonas aeruginosa* 15159 isolates were originally obtained from patients with chronic venous ulcers.

Radial diffusion assay – Radial diffusion assays (RDA) were performed essentially as described earlier (36). Briefly, bacteria were grown to mid-logarithmic phase in 10 ml of full-strength (3% w/v) trypticase soy broth (TSB) (Becton, Dickinson & Co). The microorganisms were then washed once with 10 mM Tris, pH 7.4. 4×10^6 bacterial colony forming units were added to 5 ml of the underlay agarose gel, consisting of 0.03% (w/v) TSB, 1% (w/v) low electroendosmosis type (EEO) agarose (Sigma-Aldrich, St Louis MO, USA) and 0.02% (v/v) Tween 20 (Sigma-Aldrich). The underlay was poured into a Ø 85 mm Petri dish. After agarose solidification, 4 mm-diameter wells were punched and 6 µl of test sample was added to each well. Plates were incubated at 37°C for 3 h to allow diffusion of the peptides. The underlay gel was then covered with 5 ml of molten overlay (6% TSB and 1% Low-EEO agarose in dH₂O). Antimicrobial activity of a peptide was visualized as a zone of clearance around each well after 18-24 h of incubation at 37°C. Screening for antimicrobial activity of peptides derived from domain 5 (KHN20, GHG20, GHG21, GGH20, HKH20, GKH17, all at 100 µM) was performed against *E. coli*. For comparison, we used LL-37 (100 µM) (Fig. 2B). The zones of *E. coli* clearance generated by different concentrations (10, 50, 100 µM) of rD5 and HKH20 were compared with the same concentrations of LL-37 (Fig. 2C). The dose-response characteristics of RDA were used to determine the minimal effective concentration (MEC) of HKH20 against *P. aeruginosa*. The log₁₀ concentrations of HKH20 were plotted versus the respective diameter of the zone of clearance (not shown). Linear regression using least squares was used to estimate the MEC-value, which was determined by triplicate experiments using eight serial 2-fold dilutions (starting at 512 µM) of HKH20. HMWK degradation products were tested for inhibitory effects against *E. coli* (Fig. 6A). The proteases (incubated for 1 h, at 37°C), used at equivalent concentrations as in the HMWK-degradations, were added as controls. Using RDA (*E. coli*), zones of clearance generated by LDD40 and LL-37, respectively, were compared (Fig. 6F).

Viable count analysis – *E. coli*, *E. faecalis* and *P. aeruginosa* bacteria were grown to mid-logarithmic phase in Todd-Hewitt (TH) medium. Bacteria were washed and diluted in 10 mM Tris, pH 7.4 containing 5 mM glucose. Bacteria (50 µl; 2×10^6 cfu/ml) were incubated, at 37°C for 2 hours, with rD5 protein (Fig. 2A), HKH20 (Fig. 2D) or LDD40 (Fig. 6E) peptide at concentrations indicated in the figures. To test the time-dependence of bacterial killing, 30 µM HKH20 was used against *E. faecalis* and 0.6 µM HKH20 against *P. aeruginosa* and incubations were performed for 5, 15, 30, 60 and 120 min (Fig. 3C). Activity of 10 µM HKH20 was also tested against *P. aeruginosa* diluted in 10 mM Tris, 0.15 M NaCl +/- 20% human EDTA-plasma. Significance was determined by using the Holm-Sidak method; one way repeated measures analysis of variance (ANOVA) and the statistical software used was SigmaStat, (SPSS Inc., Chicago, IL, USA) (Fig. 4).

To quantify the bactericidal activity, serial dilutions of the incubation mixtures were plated on TH agar, followed by incubation at 37°C overnight and the number of colony-forming units was determined. 100% survival was defined as total survival of bacteria in the same buffer and under the same conditions as in the absence of peptide.

Heparin-binding assay – The rD5 protein and the synthetic HKH20 peptide (1, 2, 5 µM) were applied onto nitrocellulose membranes (HybondTM-C, GE Healthcare BioSciences, Little Chalfont, United Kingdom). Membranes were blocked (phosphate buffered saline (PBS), pH 7.4, 3% bovine serum albumin) for one hour and incubated with radiolabeled heparin (¹²⁵I) (~10 µg/ml)(22). Unlabeled heparin (6 mg/ml) was added for competition of binding. The membranes were washed (3 x 10 min in 10 mM Tris, pH 7.4). A Bas 2000 radioimaging system (Fuji) was used for visualization of radioactivity.

Electron microscopy – Suspensions of *P. aeruginosa* (16×10^6 per sample) were incubated for 2 h at 37°C with the HKH20 peptide at 0.03 µM and 60 µM. For control, we included untreated bacteria. Each sample was gently transferred onto poly-L-lysine-coated Nylaflo® (GelmanSciences, MI) nylon membranes. The membranes were fixed in 2.5% (v/v) glutaraldehyde in 0.1 M sodium cacodylate, pH 7.2, for 2 h at 4°C, and subsequently washed with 0.15 M cacodylate, pH 7.2. They were then postfixed with 1% osmium tetroxide (w/v) and

0.15 M sodium cacodylate, pH 7.2, for 1 h at 4°C, washed, and subsequently dehydrated in ethanol and further processed for Epon embedding. Sections were cut with a microtome and mounted on Formvar coated copper grids. The sections were stained with uranyl acetate and lead citrate and examined in a Jeol 1200 EX transmission electron microscope operated at 60 kV accelerating voltage (Fig. 3B).

Fluorescence microscopy – *P. aeruginosa* bacteria were grown to mid-logarithmic phase in TH medium. The bacteria were washed twice in 10 mM Tris, pH 7.4. The pellet was dissolved to yield a suspension of 5×10^6 cfu/ml in the same buffer. Two hundred microliters of the bacterial suspension was incubated with 1 µg Texas Red (TR-) conjugated HKH20 on ice for 5 min and washed twice in 10 mM Tris, pH 7.4. To test if heparin inhibits the binding of peptide to bacteria, TR-HKH20 was incubated on ice for 5 min with an excess of heparin (50 µg) prior to the incubation with bacteria. The bacteria were fixed by incubation on ice for 15 min and in room temperature for 45 min in 4% paraformaldehyde. The suspension was applied onto Poly-L-lysine coated cover glass and bacteria were let to attach for 30 min. The liquid was poured away and the cover glass was mounted on a slide by Dako mounting media, Dako (Carpinteria, CA, USA). The bacteria were visualized by using a Nikon Eclipse TE300 inverted fluorescence microscope equipped with a Hamamatsu C4742-95 cooled CCD camera, a Plan Apochromat (x100 objective), and a high-numerical-aperture oil-condenser.

Hemolysis assay – EDTA-blood was centrifuged at 800 g for 10 min, plasma and buffy coat were removed. The erythrocytes were washed three times and resuspended in 5% PBS, pH 7.4. The cells were then incubated with end-over-end rotation for 1 h at 37°C in the presence of different concentrations of peptides (0, 3, 6, 30, 60 µM). 2% Triton X-100 (Sigma-Aldrich) served as positive control. The samples were then centrifuged at 800 g for 10 min. The absorbance of hemoglobin release was measured at λ 540 nm and is in the plot expressed as % of TritonX-100 induced hemolysis.

Lactate dehydrogenase (LDH) assay – HaCaT keratinocytes were grown in 96 well plates (3000 cells/well) in DMEM/10% fetal calf serum (FCS) to confluency. The medium was removed and the cells were washed with 100 µl DMEM. 100 µl of HKH20 and LL-37 (0, 3, 6, 30, 60 µM) diluted in DMEM were added in

triplicates to different wells of the plate. The LDH based TOX-7 kit (Sigma-Aldrich) was used for quantification of LDH release from the cells. For detailed laboratory procedure, see instructions given by the manufacturer.

MTT- assay – Sterile filtered MTT (3-(4,5-dimethylthiazolyl)-2,5-diphenyl-tetrazolium bromide, (Sigma-Aldrich)) solution (5 mg/ml in PBS) was stored protected from light at -20°C until usage. HaCaT keratinocytes, 3000 cells / well, were seeded in 96 well plates and grown in DMEM/10% FCS to confluency. The medium was changed to DMEM (without FCS) and HKH20 peptide was added in triplicates at different concentrations (0, 3, 6, 30, 60 µM). After over night incubation 20 µl of the MTT solution was added to each well and the plates were incubated for 1 h in CO₂ at 37°C. The MTT containing medium was then removed by aspiration. Each well was washed gently with 100 µl PBS and the blue formazan product generated was dissolved by the addition of 100 µl of 100% DMSO per well. The plates were gently swirled for 10 min at room temperature, to dissolve the precipitate. The absorbance was monitored at λ 550 nm.

Proteolytic generation of peptides from HMWK – HMWK (16 µg) was incubated at 37°C for 10 or 30 min with either *P. aeruginosa* elastase (0.1 µg, 261 u/mg) or neutrophil elastase (0.4 µg, 29 u/mg) or freeze/thaw disrupted polymorphonuclear neutrophils (PMN) (17.7 µl, 1×10^6 cells/ml) in a total volume of 30 µl. HMWK (16 µg) incubated at 37°C for 30 min was used for control. Fifteen microliters of the material were analyzed on 16.5% precast sodium dodecyl sulfate polyacrylamide (SDS-PAGE) Tris-Tricine gels (BioRad, Hercules, CA, USA) under reducing conditions (Fig. 6B). Proteins/peptides were also transferred to nitrocellulose membranes (HybondTM-C, GE Healthcare Biosciences). Membranes were blocked by 3% (w/v) skimmed milk, washed, and incubated for 1 h with rabbit polyclonal HKH20 antibodies (1:5000) (Innovagen AB), washed again, and subsequently incubated (1 h) with HRP-conjugated secondary swine anti rabbit antibodies, 1:1000 (Dako). HKH20 proteins/fragments containing whole or parts of the HKH20 sequence were visualized using the ECL developing system (GE Healthcare Biosciences) (Fig. 6C).

Definition of kininogen cleavage product – Peptides generated by degradation of HMWK by

P. aeruginosa elastase were transferred from a 16.5% Tris-Tricine gel onto PVDF membranes (HybondTM-P, GE Healthcare Bio-Sciences Biosciences). One major peptide (indicated by an arrow in Fig. 6B) was cut out and sent for N-terminal sequencing (Protein Analysis Center, Karolinska Institutet, Stockholm, Sweden). The sequence LDDDL was obtained. The major detected MALDI signal (Protein Analysis Center, Karolinska) corresponded to the mass 4428.19 Da, thus identifying the peptide as LDD40 (Fig. 6D).

RESULTS

Antimicrobial effects of recombinant domain 5 and D5 derived peptides from HMWK. To elucidate whether domain 5 of HMWK possess antibacterial activity, we initially investigated the effects of purified recombinant domain 5 (rD5) on *E. faecalis* (Fig. 2A) and *E. coli* (Fig. 2C). The results showed that rD5 was found to be antibacterial against these bacteria. Notably, rD5 exerted similar inhibitory activity in RDA as the classical AMP LL-37 (Fig. 2C). In order to characterize functional antimicrobial epitopes of this domain of HMWK, we synthesized overlapping peptides (Fig. 1B) and tested these for antibacterial activities. The results showed that peptides derived from the histidine and lysine-rich parts of D5 (H469-K502, represented by peptides GGH20, HKH20, and GKH17) exerted potent antibacterial activities in RDA against *E. coli* (Fig. 2B). The calculated pI-values for these active peptides ranged between 9.70 and 10.78 (www.expasy.org/tools/pi_tool.html), and the net positive charge was +3 to +7, values comparable to those reported for many cationic AMPs. RDA analyses using *P. aeruginosa* and *E. faecalis*, identified the HKH20 peptide as the most potent epitope of D5 (not shown) and furthermore, the HKH20 peptide exerted antimicrobial effects comparable to both intact rD5 as well as LL-37 (Fig. 2C). Likewise, molecular modeling of the rD5 sequence using the homologous protein hisactophilin from *Dictyostelium discoideum* as a template, suggested that the sequence H479-H498 expose critical cationic lysine residues, which enable interaction of rD5 with negatively charged bacterial membranes. Thus, in the following experiments, we focused on this specific epitope of D5 (Fig. 1A, B). In viable count assays, HKH20 exerted antibacterial effects against *E. coli*, *P. aeruginosa* and

E. faecalis (Fig. 2D). Using RDA, the MEC-value of HKH20 against *P. aeruginosa* was estimated to 0.4 μ M, which was comparable to the previously reported activity of LL-37 (21). As recently shown by us, a cross-functionality exist between AMPs and heparin-binding peptides (22), and this applies to classical AMPs such as LL-37 and defensin, the anaphylatoxin C3a, as well as several other heparin-binding peptides. Analogous to the studies by Pixley *et. al.* on the heparin binding of domain 5 of HMWK (28), rD5 and the HKH20 peptide bound to radiolabeled heparin at physiological salt concentrations (Fig. 2E), thus providing an additional link between rD5, HKH20, and cationic AMPs.

HKH20 binds to bacterial surfaces. The interaction between the HKH20 peptide and bacterial plasma membranes was examined by fluorescence and electron microscopy. HKH20 was labeled with the fluorescence dye Texas Red and incubated with *P. aeruginosa*. As demonstrated by fluorescence microscopy, the peptide was bound to the bacterial surface, and the binding was completely blocked by heparin (Fig. 3A, panel 2). Next, *P. aeruginosa* was incubated with HKH20 at 0.03 μ M and 60 μ M and analyzed by electron microscopy. We noted clear differences in the morphology of HKH20-treated bacteria in comparison with the control (Fig. 3B). HKH20 caused local perturbations and breaks along *P. aeruginosa* bacterial plasma membranes, and intracellular material was found extracellularly. These findings were similar to those seen after treatment with the antimicrobial peptide LL-37 (22). Most AMPs act rapidly on bacterial membranes, and thus, we next investigated the time-dependence of bacterial killing. As demonstrated in Fig. 3C, more than 80% of the Gram-negative *P. aeruginosa* were killed by 0.6 μ M HKH20 within 5 min. Longer incubation times were required for efficient killing of the Gram-positive *E. faecalis* (~50% of bacteria killed by 30 μ M peptide after 15 min).

Antibacterial activities at physiological conditions. Presence of plasma proteins and the ionic environment govern the activity of AMPs. For example, the antimicrobial activities of defensins are inhibited at physiological salt conditions (37). Thus, we examined the influence of physiological salt (0.15 M NaCl) as well as plasma on the antimicrobial activity of the HKH20 peptide. At 10 μ M HKH20 (a concentration yielding complete killing of *P. aeruginosa* in 10 mM Tris buffer), the peptide

retained its antibacterial effects in the presence of 0.15 M NaCl as well as in the presence of human plasma (20%) (Fig. 4).

Peptide effects on erythrocytes and eukaryotic cells. A number of de novo designed as well as naturally occurring AMPs exhibit various levels of lytic activity towards mammalian cells. Notably, the cathelicidin LL-37 is cytotoxic to normal eukaryotic cells and exhibits a significant degree of hemolytic activity (38). Our results showed that HKH20 exerted no hemolytic effects at 60 μ M, a concentration exceeding the estimated MEC value of this peptide. In contrast, 60 μ M LL-37 yielded approximately 10% hemolysis (Fig. 5A). rD5 as well as the other D5-derived peptides yielded similar results as HKH20 (not shown). Likewise, no permeabilization of HaCaT cells was detected in presence of 60 μ M HKH20, whereas the LL-37 peptide yielded 100% LDH release at the same concentration, indicating total disruption of the cells (Fig. 5B). In order to study potential effects on cell viability and growth, a MTT-assay was employed to measure the peptide effects on HaCaT cells. Increasing concentrations of the HKH20 peptide did not significantly affect the proliferation of HaCaT cells, whereas LL-37 showed a tendency to negatively influence cell growth (Fig. 5C).

Proteolytic cleavage of HMWK generates antimicrobial peptides. Intact HMWK exerted no antimicrobial effects (Fig. 6A, sample #4). Thus, we investigated whether antimicrobial and D5-derived peptides could be released after proteolytic digestion of HMWK. Thus, HMWK was incubated with the serine protease elastase from human neutrophils (HLE), extracts of neutrophils (PMN), as well as the bacterial metalloproteinase elastase (PAELA) of *P. aeruginosa*. The results showed the degraded HMWK indeed generated zones of inhibition in RDA against *E. coli* (Fig. 6A). SDS-PAGE analysis of the peptides generated revealed that HMWK was extensively degraded into multiple fragments. Notably, *P. aeruginosa* elastase as well as the neutrophil extract yielded low molecular weight peptides after a 30 min incubation time. Western blot analysis using an HKH20 antibody demonstrated that several immunoreactive fragments were generated. Notably, *P. aeruginosa* elastase generated one major peptide of an apparent molecular mass of ~7 kDa, and a similar peptide was observed after treatment with the neutrophil extracts (Fig. 6C). The major HKH20-reactive D5-fragment

generated after digestion with *P. aeruginosa* elastase (Fig. 6B, black arrow) was analyzed by Edman degradation and MALDI-TOF analysis. The results yielded a 40 aa peptide sequence, LDD40 (L461-G500) (Fig. 6D). Interestingly, HKH20 constituted the major part of the C-terminus of the LDD40 peptide. The LDD40 peptide was synthesized and found to be antibacterial against *E. faecalis* (Fig. 6E) and *E. coli* (Fig. 6F).

DISCUSSION

The main findings in our study is the identification of a potent antibacterial activity of recombinant domain 5 and the corresponding characterization of antimicrobial D5-derived peptides from HMWK, in concert with a conceptual proof that similar antibacterial epitopes are generated during proteolysis of HMWK *in vitro*. The results have implications for our understanding of novel properties of HMWK, and will enable future development of D5-derived AMPs for therapeutic use.

The D5 domain is multifunctional, and binds cellular receptors (29,39-41) as well as anionic surfaces (42), and inhibits angiogenesis by inducing apoptosis of proliferating endothelial cells (30). From a structural perspective, several lines of evidence indicate that the epitope involving the sequence H479-H498 of D5 is responsible for its antimicrobial activity. Although tentative, molecular homology modeling studies suggest that HKH20 is found at the surface of the domain 5 (Fig. 1A, yellow in upper panel). Thus, positively charged lysine residues of HKH20 (Fig. 1A, red in upper panel), protruding outward from the molecule have the capacity to interact with negatively charged structures, such as bacterial plasma membranes as well as heparin (Fig. 3A, Fig. 2E). Interestingly, HKH20 as well as GKH17 contains the consensus sequence for heparin binding, XBBXB_X (in reverse; ⁴⁹⁰NKGKKN^{†495}, where X represents hydrophobic or uncharged amino acids, and B represents basic amino acids) (43), peptide motifs which were recently found to exert potent antibacterial activities (22). It is also of note that domain 5 of HMWK contains two subdomains, one His-Gly-rich (K420-D474) and one His-Gly-Lys-rich (G475-K502), the latter including HKH20 (Fig. 1A, B). Whereas, the heparin-binding capacity of the His-Gly-rich domain is Zn²⁺ dependent, the His-Gly-Lys-rich part is able to bind heparin regardless of Zn²⁺

(28). Results with rD5 as well as HKH20 yielded similar antimicrobial activities in absence or presence of 50 μM Zn^{2+} (not shown). Likewise, heparin completely abolished the antimicrobial activity of both molecules, suggesting that the lysine-rich, and Zn^{2+} -independent domain comprising HKH20 is sufficient for the antimicrobial activity of the D5 domain.

The observation that insects and mammals utilize AMPs to counter microbial infections has, in combination with the growing problem of resistance to conventional antibiotics, spawned considerable interest in the discovery and subsequent development of novel AMPs for therapeutic use. Various strategies, (for reviews see (44,45) such as use of combinational library approaches, stereoisomers composed of D-amino acids or cyclic D,L- α -peptides are employed in the development of therapeutically interesting AMPs. Due to potential lytic properties of AMPs against bacterial as well as mammalian membranes, one of the challenges in designing new peptides relies on developing AMPs with high specificity against bacterial or fungal cells, i.e., a high therapeutic index (minimal hemolytic concentration/minimal antimicrobial activity; MHC/MEC). The finding that D5, as well as HKH20 displayed no lytic activities against mammalian cells, suggest a high amount of dissociation between antimicrobial and antieukaryotic activities. Biomembranes are highly complex structures, and currently, efforts are undertaken to gain a deeper understanding of the complex structure-activity relationships governing AMP specificity and selectivity (44,45). However, factors such as high hydrophobicity, α -helicity, as well as tendency to self-associate are linked to high hemolytic activity (as exemplified by our results with LL-37). The structural prerequisites for the selectivity and exact antimicrobial action of HKH20 remain to be characterized, however, the peptide has some unique features, such as high net charge, absence of hydrophobic residues, and a high amount of lysine and histidine, separating it from the group of classical helical amphipathic AMPs. The peptide exerted similar membrane breaking effects as LL-37. Analogously, recent studies indicate that the peptide, displaying random conformation in aqueous solutions, has a high specificity against negatively charged artificial liposomes, and little effects on zwitterionic membranes², thus in agreement with the herein noted bacterial specificity. Interestingly, *P. aeruginosa*, *E. faecalis*, *Proteus*

mirabilis, *Streptococcus pyogenes* (46) and *Staphylococcus aureus* (47) all secrete proteases that degrade the cathelicidin LL-37. Unlike LL-37, HKH20 is highly resistant to various bacterial proteases (not shown), likely due to absence of hydrophobic residues in HKH20. Notably, the *P. aeruginosa* elastase, *E. faecalis* gelatinase, or 50 kDa metalloproteinase of *P. mirabilis* belong to the M4 peptidase family (thermolysin family) and have similar specificities requiring hydrophobic amino acids (L, I, F) at the P1' position (48,49). Taken together, from a therapeutic standpoint, our results suggest that strategies based on utilizing endogenous, and protease-resistant, AMPs with a high therapeutic index could be highly rewarding.

From a biological perspective, it is well established that HMWK is proteolytically processed by endogenous as well as bacterial proteases, leading to release of different immunomodulating and bioactive peptides (for reviews see (24,26,50). During contact activation plasma kallikrein cleaves out the proinflammatory nanopeptide bradykinin from HMWK. In addition, mast cell tryptase and neutrophil elastase are both able to release a vascular permeability enhancing peptide (E-kinin) containing the bradykinin peptide (51,52). Furthermore, kinins may be released by cysteine proteinases of *Porphyromonas gingivalis* and of *Streptococcus pyogenes* (50,53,54).

The data presented in this study provide a first proof of concept that D5-derived antibacterial fragments comprising the HKH20 epitope are generated after proteolysis of HMWK. This observation was further substantiated by the structural characterization of a proteolytically generated and antimicrobial peptide fragment, LDD40, generated by elastase from *P. aeruginosa* (Fig. 6B, D, E, F). The observation that an bacterial elastase as well as endogenous neutrophil-derived proteases yielded similar HKH-containing fragments of domain 5 not only reflect the protease-resistance of this domain (as discussed above), but also suggests that this generation may reflect a common mechanism for generation of antimicrobial peptides from this domain *in vivo*. Highly relevant to our results, findings by other investigators indicate that AMPs derived from other parts of HMWK indeed may be generated. For example, apart from D5, bradykinin of domain 4 was found to possess antimicrobial activities (15). Furthermore, results at our

laboratory indicate that vascular permeability enhancing peptide (E-kinin), SLMKRPPGFS-PFRSSRI, containing the bradykinin peptide (51,52) generated by the concerted actions of mast cell tryptase and neutrophil elastase is also antimicrobial against both *P. aeruginosa* and *S. aureus* (not shown). Taken together, these findings indicate that multiple AMPs may be proteolytically released from HMWK. As illustrated in Fig. 6C, a mixture of neutrophil proteases generated low-molecular weight HKH20-like peptides, whereas neutrophil elastase yielded larger D5-derived fragments.

This illustrates that multiple processing steps induced by the concerted action of various proteases on HMWK are likely to occur *in vivo*. Interestingly, an analogous processing has indeed been described for the cathelicidin LL-37 (55), yielding enhanced antibacterial activities of the resulting peptide fragments. Thus, current investigations aim at characterizing D5-derived AMPs that are generated during various inflammatory and infective processes *in vivo*, their resulting antimicrobial activities, and roles in innate immunity.

REFERENCES

1. Zeya, H. I., and Spitznagel, J. K. (1963) *Science* **142**, 1085-1087
2. Steiner, H., Hultmark, D., Engström, A., Bennich, H., and Boman, H. G. (1981) *Nature* **292**, 246-248
3. Zasloff, M. (1987) *Proc. Natl. Acad. Sci. U S A* **84**, 5449-5453
4. Elsbach, P. (2003) *J. Clin. Invest.* **111**, 1643-1645
5. Zanetti, M. (2004) *J. Leukoc. Biol.* **75**, 39-48
6. Agerberth, B., Charo, J., Werr, J., Olsson, B., Idali, F., Lindbom, L., Kiessling, R., Jörnvall, H., Wigzell, H., and Gudmundsson, G. H. (2000) *Blood* **96**, 3086-3093
7. De, Y., Chen, Q., Schmidt, A. P., Anderson, G. M., Wang, J. M., Wooters, J., Oppenheim, J. J., and Chertov, O. (2000) *J. Exp. Med.* **192**, 1069-1074
8. Territo, M. C., Ganz, T., Selsted, M. E., and Lehrer, R. (1989) *J. Clin. Invest.* **84**, 2017-2020
9. Yoo, Y. C., Watanabe, R., Koike, Y., Mitobe, M., Shimazaki, K., Watanabe, S., and Azuma, I. (1997) *Biochem. Biophys. Res. Commun.* **237**, 624-628
10. Ciornei, C. D., Egesten, A., and Bodelsson, M. (2003) *Acta Anaesthesiol. Scand.* **47**, 213-220
11. Okumura, K., Itoh, A., Isogai, E., Hirose, K., Hosokawa, Y., Abiko, Y., Shibata, T., Hirata, M., and Isogai, H. (2004) *Cancer Lett.* **212**, 185-194
12. Li, J., Post, M., Volk, R., Gao, Y., Li, M., Metais, C., Sato, K., Tsai, J., Aird, W., Rosenberg, R. D., Hampton, T. G., Sellke, F., Carmeliet, P., and Simons, M. (2000) *Nat. Med.* **6**, 49-55
13. Koczulla, R., Von Degenfeld, G., Kupatt, C., Krotz, F., Zahler, S., Gloe, T., Issbrucker, K., Unterberger, P., Zaiou, M., Leberherz, C., Karl, A., Raake, P., Pfosser, A., Boekstegers, P., Welsch, U., Hiemstra, P. S., Vogelmeier, C., Gallo, R. L., Clauss, M., and Bals, R. (2003) *J. Clin. Invest.* **111**, 1665-1672
14. Cole, A. M., Ganz, T., Liese, A. M., Burdick, M. D., Liu, L., and Strieter, R. M. (2001) *J. Immunol.* **167**, 623-627
15. Brogden, K. A., Guthmiller, J. M., Salzet, M., and Zasloff, M. (2005) *Nat. Immunol.* **6**, 558-564
16. Kowalska, K., Carr, D. B., and Lipkowski, A. W. (2002) *Life Sci.* **71**, 747-750
17. Goumon, Y., Lugardon, K., Kieffer, B., Lefevre, J. F., Van Dorselaer, A., Aunis, D., and Metz-Boutigue, M. H. (1998) *J. Biol. Chem.* **273**, 29847-29856
18. Shimizu, M., Shigeri, Y., Tatsu, Y., Yoshikawa, S., and Yumoto, N. (1998) *Antimicrob. Agents Chemother.* **42**, 2745-2746
19. Vouldoukis, I., Shai, Y., Nicolas, P., and Mor, A. (1996) *FEBS Lett.* **380**, 237-240
20. Mor, A., Amiche, M., and Nicolas, P. (1994) *Biochemistry* **33**, 6642-6650
21. Nordahl, E. A., Rydengård, V., Nyberg, P., Nitsche, D. P., Mörgelin, M., Malmsten, M., Björck, L., and Schmidtchen, A. (2004) *Proc. Natl. Acad. Sci. U S A* **101**, 16879-16884
22. Andersson, E., Rydengård, V., Sonesson, A., Mörgelin, M., Björck, L., and Schmidtchen, A. (2004) *Eur. J. Biochem.* **271**, 1219-1226
23. Park, P. W., Pier, G. B., Hinkes, M. T., and Bernfield, M. (2001) *Nature* **411**, 98-102
24. Colman, R. W., and Schmaier, A. H. (1997) *Blood* **90**, 3819-3843

25. Schmaier, A. H., Zuckerberg, A., Silverman, C., Kuchibhotla, J., Tuszyński, G. P., and Colman, R. W. (1983) *J. Clin. Invest.* **71**, 1477-1489
26. Kaplan, A. P., Joseph, K., and Silverberg, M. (2002) *J. Allergy. Clin. Immunol.* **109**, 195-209
27. Kozik, A., Moore, R. B., Potempa, J., Imamura, T., Rapala-Kozik, M., and Travis, J. (1998) *J. Biol. Chem.* **273**, 33224-33229
28. Pixley, R. A., Lin, Y., Isordia-Salas, I., and Colman, R. W. (2003) *J. Thromb. Haemost.* **1**, 1791-1798
29. Hasan, A. A., Cines, D. B., Herwald, H., Schmaier, A. H., and Müller-Esterl, W. (1995) *J. Biol. Chem.* **270**, 19256-19261
30. Zhang, J. C., Claffey, K., Sakthivel, R., Darzynkiewicz, Z., Shaw, D. E., Leal, J., Wang, Y. C., Lu, F. M., and McCrae, K. R. (2000) *Faseb J.* **14**, 2589-2600
31. Ohkubo, I., Kurachi, K., Takasawa, T., Shiokawa, H., and Sasaki, M. (1984) *Biochemistry* **23**, 5691-5697
32. Herwald, H., Mörgelin, M., Svensson, H. G., and Sjöbring, U. (2001) *Eur. J. Biochem.* **268**, 396-404
33. Habazettl, J., Gondol, D., Wiltscheck, R., Otlewski, J., Schleicher, M., and Holak, T. A. (1992) *Nature* **359**, 855-858
34. Colman, R. W., Jameson, B. A., Lin, Y., Johnson, D., and Mousa, S. A. (2000) *Blood* **95**, 543-550
35. Jacobson, M. P., Pincus, D. L., Rapp, C. S., Day, T. J., Honig, B., Shaw, D. E., and Friesner, R. A. (2004) *Proteins* **55**, 351-367
36. Lehrer, R. I., Rosenman, M., Harwig, S. S., Jackson, R., and Eisenhauer, P. (1991) *J. Immunol. Methods* **137**, 167-173
37. Ganz, T. (2001) *Semin. Respir. Infect.* **16**, 4-10
38. Oren, Z., Lerman, J. C., Gudmundsson, G. H., Agerberth, B., and Shai, Y. (1999) *Biochem. J.* **341**, 501-513
39. Wachtfogel, Y. T., DeLa Cadena, R. A., Kunapuli, S. P., Rick, L., Miller, M., Schultze, R. L., Altieri, D. C., Edgington, T. S., and Colman, R. W. (1994) *J. Biol. Chem.* **269**, 19307-19312
40. Colman, R. W., Pixley, R. A., Najamunnisa, S., Yan, W., Wang, J., Mazar, A., and McCrae, K. R. (1997) *J. Clin. Invest.* **100**, 1481-1487
41. Herwald, H., Dedio, J., Kellner, R., Loos, M., and Müller-Esterl, W. (1996) *J. Biol. Chem.* **271**, 13040-13047
42. DeLa Cadena, R. A., and Colman, R. W. (1992) *Protein Sci.* **1**, 151-160
43. Cardin, A. D., and Weintraub, H. J. (1989) *Arteriosclerosis* **9**, 21-32
44. Tossi, A., Sandri, L., and Giangaspero, A. (2000) *Biopolymers* **55**, 4-30
45. Blondelle, S. E., and Lohner, K. (2000) *Biopolymers* **55**, 74-87
46. Schmidtchen, A., Frick, I. M., Andersson, E., Tapper, H., and Björck, L. (2002) *Mol. Microbiol.* **46**, 157-168
47. Sieprawska-Lupa, M., Mydel, P., Krawczyk, K., Wojcik, K., Puklo, M., Lupa, B., Suder, P., Silberring, J., Reed, M., Pohl, J., Shafer, W., McAleese, F., Foster, T., Travis, J., and Potempa, J. (2004) *Antimicrob. Agents Chemother.* **48**, 4673-4679
48. Rozalski, A., Sidorczyk, Z., and Kotelko, K. (1997) *Microbiol. Mol. Biol. Rev.* **61**, 65-89
49. de Kreijl, A., Venema, G., and van den Burg, B. (2000) *J. Biol. Chem.* **275**, 31115-31120
50. Imamura, T., Potempa, J., and Travis, J. (2004) *Biol. Chem.* **385**, 989-996
51. Imamura, T., Dubin, A., Moore, W., Tanaka, R., and Travis, J. (1996) *Lab. Invest.* **74**, 861-870
52. Imamura, T., Tanase, S., Hayashi, I., Potempa, J., Kozik, A., and Travis, J. (2002) *Biochem. Biophys. Res. Commun.* **294**, 423-428
53. Imamura, T., Pike, R. N., Potempa, J., and Travis, J. (1994) *J. Clin. Invest.* **94**, 361-367
54. Herwald, H., Collin, M., Müller-Esterl, W., and Björck, L. (1996) *J. Exp. Med.* **184**, 665-673
55. Murakami, M., Lopez-Garcia, B., Braff, M., Dorschner, R. A., and Gallo, R. L. (2004) *J. Immunol.* **172**, 3070-3077

FOOTNOTES

* This work was supported by grants from the Swedish Research Council (projects 13471), the Royal Physiographic Society in Lund, the Welander-Finsen, Söderberg, Groschinsky, Crafoord, Alfred Österlund, Lundgrens, Lions and Kock Foundations, DermaGen AB, and The Swedish Government Funds for Clinical Research (ALF).

¹The abbreviations used are: AMP, antimicrobial peptide; HMWK, high molecular weight kininogen; rD5, recombinant domain 5; TR, PAELA, *Pseudomonas aeruginosa* elastase; HLE, human leukocyte elastase; RDA, radial diffusion assays; TSB, trypticase soy broth; EEO, electroendosmosis type; TH, Todd-Hewitt; PBS, phosphate buffered saline; LDH, lactate dehydrogenase; PMN, polymorphonuclear neutrophils.

²Ringstad, L., Schmidtchen, A., and Malmsten, M. Effects of peptide length on the activity of a kininogen-derived antimicrobial peptide on lipid bilayers, bacteria and cells, manuscript in preparation

Acknowledgement:

We wish to thank Ms Maria Baumgarten and Ms Mina Davoudi for their expert technical assistance and Dr. Björn Walse for the molecular model of domain 5.

FIGURE LEGENDS

Fig. 1. Molecular model and sequence of recombinant domain 5 and corresponding overlapping peptides. *A*, upper part, Homology model of rD5 (residues 414-525) showing the HKH20 peptide in yellow, with some of its positively charged lysine residues in red protruding outward from the molecule. The model was based on hisactophilin from *Dictyostelium discoideum* (33). The modeling was performed using the alignment described by Colman (34) and the Prime module (35) from the Schrödinger computational chemistry suite of programs (Schrödinger, L.L.C., Portland, OR, USA). *A*, lower part, The amino acid sequence of rD5. *B*, The sequences of the overlapping peptides from D5 used in this study.

Fig. 2. Activities of rD5 and D5-derived peptides. *A*, In viable count assays antibacterial activities for rD5 were detected against *E. faecalis* (—▼—). 2×10^6 cfu/ml of bacteria were incubated in 50 μ l with peptides at concentrations ranging 0.3 to 100 μ M. *B*, *C*, Peptides and rD5 protein were tested in RDA in low-salt conditions. *E. coli* (4×10^6 cfu) was inoculated in 0.1% TSB agarose gel. Each 4 mm-diameter well was loaded with 6 μ l of peptide at 100 μ M in *B* and at the indicated concentrations in *C*. The zones of clearance correspond to the inhibitory effect of each peptide after incubation at 37 °C for 18-24 h. Negative controls (labeled Ctr in *B*, and at the top left of the plate in *C*) containing buffer (10 mM Tris, pH 7.4) were included. These clear zones correspond to the 4 mm well. *D*, In viable count assays antibacterial activities for HKH20 were seen against *E. faecalis* (—▼—), *P. aeruginosa* (—○—) and *E. coli* (—●—). 2×10^6 cfu/ml of bacteria were incubated in 50 μ l with peptides at concentrations ranging from 0.03 to 60 μ M. *E*, rD5 and HKH20 were both able to bind heparin. 1, 2 and 5 μ g HKH20 were applied to nitrocellulose membranes. These membranes were then incubated in PBS (containing 3% bovine serum albumin) with iodinated (¹²⁵I) heparin. Unlabeled heparin (6 mg/ml) (+) was added for competition of binding. The membranes were washed (3 x 10 min in 10 mM Tris, pH 7.4). A Bas 2000 radioimaging system (Fuji) was used for visualization of radioactivity.

Fig. 3. Interactions of HKH20 with bacterial plasma membranes and kinetics for bacterial killing. *A*, Binding of Texas Red-labeled HKH20 to *P. aeruginosa* and inhibition of binding by excess of heparin. Image 2 shows red fluorescence of TR-HKH20 peptide (10 μ g/ml) bound to bacteria (1×10^7 /ml) and image 4 shows bacteria incubated with heparin and TR-HKH20. Images in 2 and 4

were recorded using identical instrument settings. The corresponding Nomarski images are shown in image 1 and 3. Scale bar represents 10 μm . *B*, *P. aeruginosa* (16×10^6 per sample), (left panel) was incubated for 2 h at 37°C with 0.03 μM (middle panel), and 60 μM (right panel) HKH20 and analyzed with electron microscopy. Scale bar represents 0.5 μm . *C*, The time-dependence of bacterial killing by HKH20 was analyzed by viable count assays. Concentrations of HKH20 used were 0.6 μM and 30 μM against *P. aeruginosa* (—○—) and *E. faecalis* (—▼—), respectively.

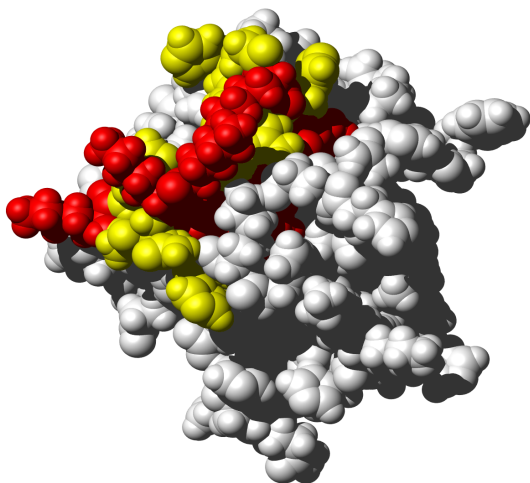
Fig. 4. Antibacterial activities of HKH20 under physiological conditions. *P. aeruginosa* bacteria were subjected to 10 μM HKH20 in 10 mM Tris pH 7.4 containing 0.15 M NaCl in presence or absence of 20% human EDTA-plasma. Identical buffers without peptide were used as controls. Significance was determined by using the Holm-Sidak method; one way repeated measures analysis of variance (ANOVA) and the statistical software used was SigmaStat, (SPSS Inc., Chicago, IL) $P < 0.001$ (***).

Fig. 5. Effects of HKH20 against eukaryotic cells. The activities of HKH20 (—●—) in the three different assays were compared with the effects of LL-37 (—○—) used at the same concentrations. The plotted values are mean out of three measurements and the error bars represent the standard deviation. *A*, Hemolytic effects of HKH20 and LL-37 were investigated. The cells were incubated with different concentrations of HKH20 or LL-37. 2% Triton X-100 (Sigma-Aldrich) served as positive control. The absorbance of hemoglobin release was measured at λ 540 nm and is expressed as % of TritonX-100 induced hemolysis (note the scale of the y-axis). *B*, HaCaT keratinocytes were subjected to HKH20 and LL-37. Cell permeabilizing effects were measured by the LDH based TOX-7 kit (Sigma-Aldrich). LDH release from the cells was monitored at λ 490 nm and was plotted as % of total LDH release. *C*, The MTT-assay was used to measure proliferation of HaCaT keratinocytes in the presence of different concentrations of HKH20 and LL-37. In the assay, MTT is modified into a dye, blue formazan, by enzymes associated with metabolic activity. The absorbance of the dye was measured at λ 550 nm.

Fig. 6. Generation of antimicrobial peptides by degradation of HMWK. *A*, Inhibitory effects of HMWK cleavage products were visualized as zones of bacterial clearance in RDA. Cleavages of HMWK were performed for 10 and 30 min at 37°C (see experimental procedures). 1: Control, *P. aeruginosa* elastase (PAELA); 2: Control, Human leukocyte (neutrophil) elastase (HLE); 3: Control, polymorphonuclear neutrophils (PMN); 4: Control, HMWK; 5 and 6: HMWK incubated with PAELA for 10 and 30 min, respectively, 7 and 8: HMWK incubated with HLE for 10 and 30 min, respectively, 9 and 10, HMWK incubated with PMN for 10 and 30 min, respectively. RDA was performed in low-salt conditions. *E. coli* (4×10^6 cfu) was used as test organism. Each 4 mm-diameter well was loaded with 6 μl . A negative control, containing buffer (10 mM Tris, pH 7.4) was included in the well at the top left of the plate. *B*, Intact HMWK (HMWK) and cleavage products from the different incubations (indicated above) were analyzed by SDS-PAGE (16.5% Tris-Tricine gel). The black arrow indicates the fragment analyzed by N-terminal sequencing and MALDI-TOF analysis. Molecular mass markers are indicated to the left. *C*, Western blot analysis identified cleavage products recognized by polyclonal antibodies against HKH20. The white arrow indicates the size of the HKH20 peptide. *D*, The indicated fragment (black arrow) in *B* was analysed by N-terminal sequencing and MALDI-TOF. *E*, Antibacterial activity of LDD40 in viable count assay. 2×10^6 cfu/ml of *E. faecalis* bacteria were incubated in 50 μl with the peptide at concentrations ranging 0.03 to 60 μM . *F*, Inhibitory effects of LDD40, compared with effects of LL-37, used at indicated concentrations against *E. coli* (4×10^6 cfu). RDA was performed in low-salt conditions. Each 4 mm-diameter well was loaded with 6 μl . A negative control, containing buffer (10 mM Tris, pH 7.4) was included in the well at the top left of the plate. A representative experiment out of six was shown.

Figure 1

A



rD5: \square 383 TVSP PHTSMA \square PAQDEERDSG \square KEQGHTRRHD
 \square \square WGHEKQRKHN \square LGHG HKHERD \square QGHGHQRGHG
 \square \square LGHGHEQQHG \square LGHG HKFKLD \square DDLEHQGGHV
 \square \square LDHG HKHKHG \square HGHG KHKNKG \square KKNKGKHNWK
 \square \square TEHLASSED \square S⁵¹³

B

KHN20: \square ⁴²⁰ KHNLGHG HKH \square ERDQGHGHQR⁴³⁹
GHG20: \square ⁴⁴⁰ GHGLGHGHEQ \square QHGLGHG HKF⁴⁵⁹
GHG21: \square ⁴⁵⁴ GHG HKFKLDD \square DLEHQGGHVLD⁴⁷⁴
GGH20: \square ⁴⁶⁹ GGHVLDHG HK \square HKHGHG HKH⁴⁸⁸
HKH20: \square ⁴⁷⁹ HKHGHG HKH \square KNKGKKNKGK⁴⁹⁸
GKH17: \square ⁴⁸⁶ GKHKKNKGKKN \square GKHNWK⁵⁰²

Figure 2

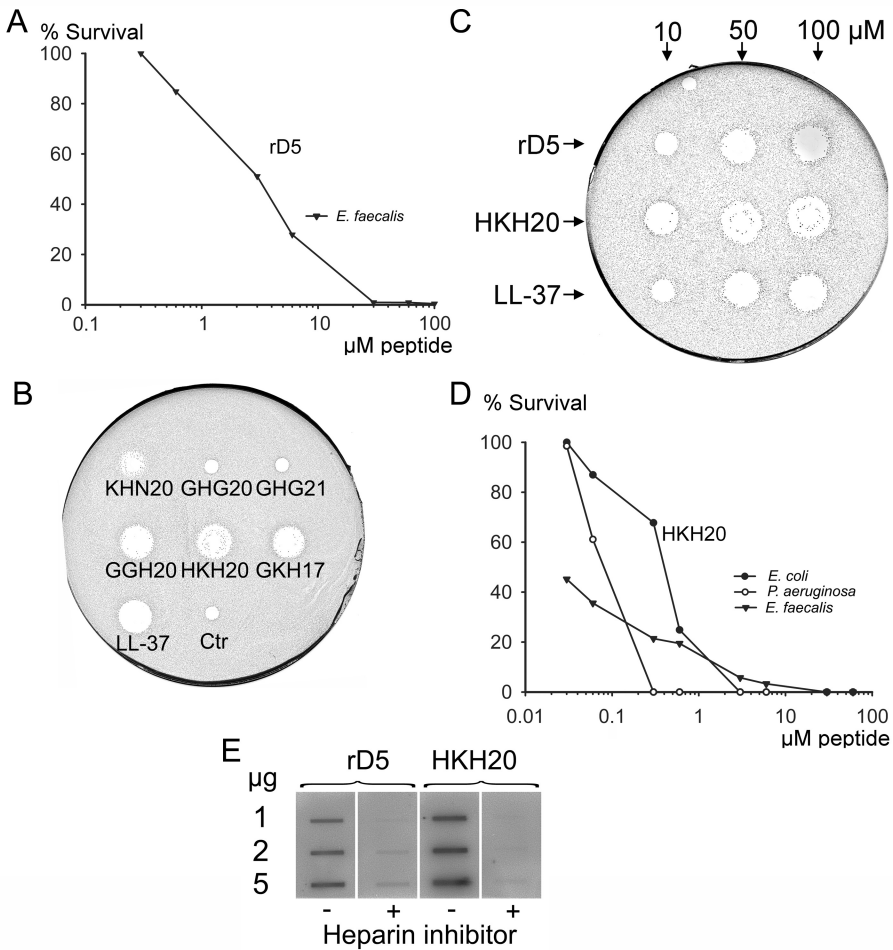


Figure 3

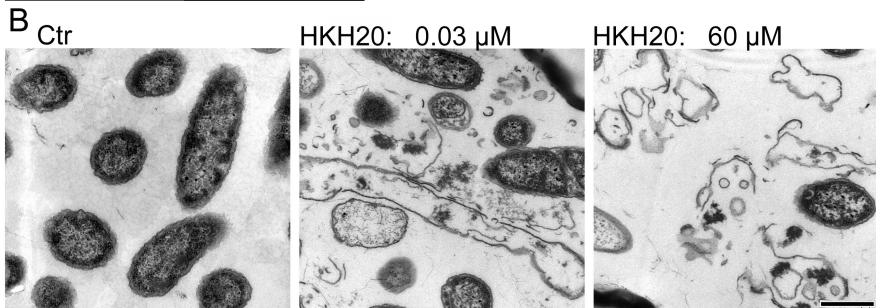
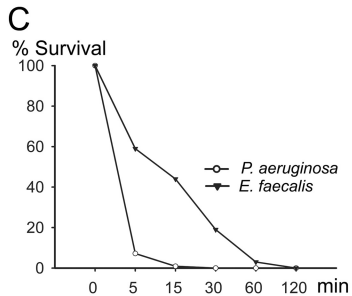
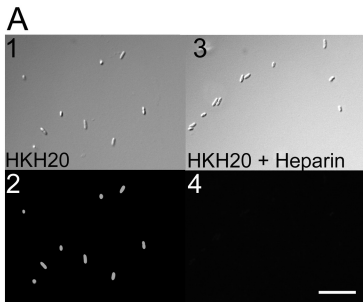


Figure 4

% Survival

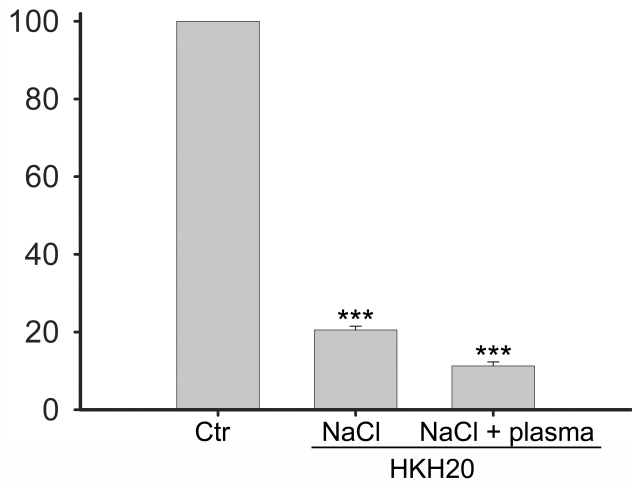


Figure 5

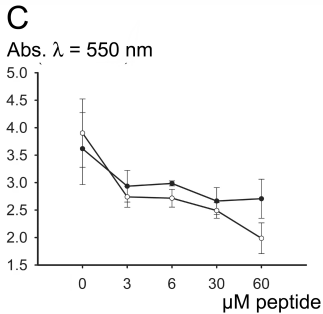
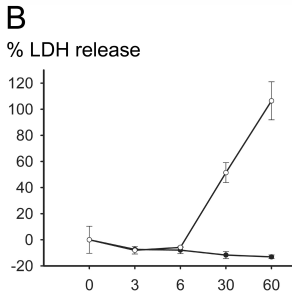
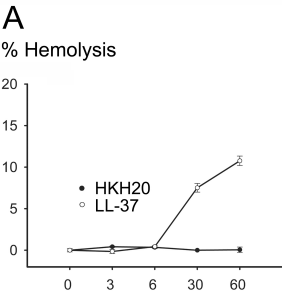
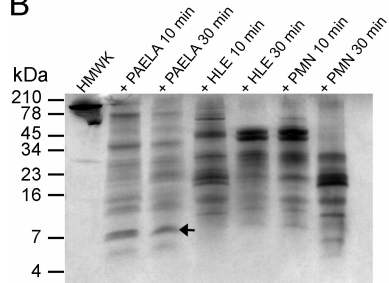


Figure 6

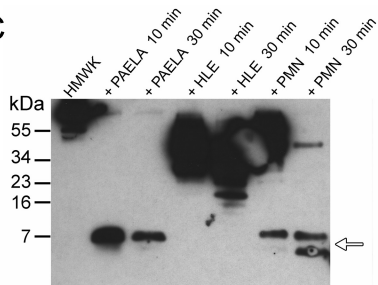
A



B



C

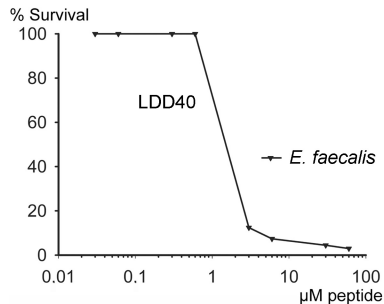


D

LDD40:

⁴⁶¹LDDDDLEHQGG HVLDDHGKHKH
HGHGKHKHKN KGKKNKGKHN⁵⁰⁰

E



F

